Slowing-down of Fast Ions in a Plasma: Energy Transfer, Charge Exchange Losses and Wall Sputtering.

W. Ott, E. Speth, A. Stäbler

IPP 4/161 July 1977

MAX-PLANCK-INSTITUT FÜR PLASMAPHYSIK

8046 GARCHING BEI MÜNCHEN

MAX-PLANCK-INSTITUT FÜR PLASMAPHYSIK

GARCHING BEI MÜNCHEN

Slowing-down of Fast Ions in a Plasma: Energy Transfer, Charge Exchange Losses and Wall Sputtering.

W. Ott, E. Speth, A. Stäbler

IPP 4/161 July 1977

Die nachstehende Arbeit wurde im Rahmen des Vertrages zwischen dem Max-Planck-Institut für Plasmaphysik und der Europäischen Atomgemeinschaft über die Zusammenarbeit auf dem Gebiete der Plasmaphysik durchgeführt.

IPP 4/161

Slowing-down of Fast Ions in a Plasma: Energy Transfer, Charge Exchange Losses and Wall Sputtering

W. Ott, E. Speth, A. Stäbler

July 1977

Abstract

Slowing-down of fast ions created by neutral injection into a tokamak plasma is investigated in order to determine the energy transferred to the ions and electrons of the plasma and the losses of particles and energy caused by charge exchange with the background neutrals. The impurity influx produced by wall-sputtering of the lost particles is calculated taking into account the energy dependent sputtering coefficient for hydrogen on stainless steel. Since energy transfer and charge exchange losses strongly depend on the neutral density and the electron temperature, the allowance of arbitrary profiles for (n_o/n_e) and T_e as well as for the fast ion deposition is incorporated. Several applications of the derived formalism are given for the case of the ASDEX tokamak.

I. INTRODUCTION

The injection of fast neutral atoms has proved to be one of the most promising methods for the additional heating of present day tokamak plasmas. The heating effect is due to the collisional energy transfer from the fast ions borne on confined orbits to the plasma particles. This fast ion slowing-down was, experimentally, found to be in good agreement with classical beam-plasma interaction /1/. The energy transferred to the plasma, however, may be seriously affected by charge exchange between fast ions and neutral background particles. One of the purposes of this work was to calculate the particle losses, the associated energy losses and the impurity influx caused by wall-sputtering of the fast neutrals. These effects are shown to be strongly depending on the relation: neutral background density to electron density (n_o/n_e). Since (n_o/n_e) usually increases with the plasma radius by more than one order of magnitude, the calculations are extended in order to take into account given profiles of (n_o/n_e) and T_e as well as an arbitrary fast ion deposition profile. The losses and the resulting impurity influx are then determined by integrating over the plasma cross section.

The fraction of the injected energy given up to the plasma ions and electrons, respectively, will be investigated in a second part. Formulae for the radial heating power density as well as for the total heating power for both, ions and electrons are derived. Charge exchange losses and the allowance of arbitrary profiles are included in these calculations, too.

II. BASIC PROCESSES

II.1 Slowing-down of fast ions

The following formulae derived by Stix /2/ will be used to describe the slowing-down time τ_o of the fast ions from their initial energy E_o to thermal energies $T_i \ll E_o$:

$$\tau_o = \frac{t_s}{3} \ln \{ 1 + (E_o/E_c)^{3/2} \} \qquad \text{(II.1)}$$

with

$$t_s = 6.27 \times 10^8 \frac{T_e^{3/2}}{\ln \Lambda \cdot n_e} \cdot \frac{A}{Z^2} \qquad \text{(II.2)}$$

$$E_c = 14.8\, T_e \{ \frac{A^{3/2}}{n_e} \sum_j \frac{n_j Z_j^2}{A_j} \}^{2/3} = 14.8\, T_e \{ \frac{A^{3/2}}{A_i} [Z] \}^{2/3} \qquad \text{(II.3)}$$

(T_e in eV, n_e in cm^{-3}, A, Z: mass and charge number of the fast ions, A_j, Z_j: mass and charge number of the plasma ions; the index i indicates the dominant plasma species). Here, t_s corresponds to the Spitzer ion-electron slowing-down time and E_c is the so-called "critical" energy, where the differential energy transfer to the ions equals that to the electrons. For a plasma with only one dominant ion species and not too high Z_{eff} the following relation holds: $[Z] = (1/n_e) * \sum_j n_i Z_j^2 * (A_i/A_j) \simeq 1$. This means that E_c and the slowing-down time τ_o depend only very weakly on the plasma impurity level. In all numerical calculations, therefore, [Z]= 1 was assumed.

From eq. (II.1) the time behaviour of the fast ion energy ("slowing--down velocity") may be deduced:

$$\frac{dE}{dt} = - \frac{2E}{t_s} \{ 1 + (E_c/E)^{3/2} \} \qquad (II.4)$$

The functions $\tau_o = f(E_o)$ and $(dE/dt) = f(E)$ are displayed for several values of the electron temperature in Fig. 1, assuming H^o-injection into a hydrogen plasma ($A = A_i = 1$). The slowing-down velocity exhibits a minimum at $E = 2^{-2/3} * E_c$ in the case of $A = A_i = 1$, this minimum occurs at $E \simeq 10 * T_e$.

II.2 Charge Exchange

For a given neutral background density n_o, the loss rate of fast ions with velocity v, caused by charge exchange (CX) is determined by:

$$\frac{dN}{dt} = - \sigma(v) \; v \; n_o \; N(t) = - \sigma(E/A) \; v \; n_o \; N(t) \qquad (II.5)$$

where N(t) denotes the time dependent number of fast ions with velocity v. Here, it is assumed that v is large compared to the neutral particle velocity. The calculations of the following sections are restricted to the injection of hydrogen isotopes (Z = 1) into a plasma whose dominant species consists of hydrogen isotopes, too. The relevant CX-cross section (e.g. $\underline{H^+} + H^o \rightarrow \underline{H^o} + H^+$) is taken according to Riviere /3/:

$$\sigma(E/A) = \frac{0.6937 * 10^{-14} \; (1.0 - 0.155 \; \log_{10} (E/A))^2}{1.0 + 0.1112 * 10^{-14} \cdot (E/A)^{3.3}} \; cm^2 \qquad (II.6)$$

E/A (in eV) is the energy per nucleon of the fast particles.

III. CHARGE EXCHANGE LOSSES AND IMPURITY INFLUX FOR CONSTANT PLASMA PARAMETERS

III.1 Particle Losses

Since we are interested in the energy dependence (not in the time dependence) of the fast ion number, the following equations should be understood as the result of summation over one neutral beam pulse. $N_o \equiv N(E_o)$ gives the number of fast ions with initial energy E_o created during one pulse duration. In calculating N(E), the number of fast ions which are still present at energy E ($E_o > E > T$), it is assumed that, firstly all fast neutrals produced by CX-processes will escape from the plasma and, secondly that this process is the only loss mechanism for the fast ions. Taking eqs. (II.4) and (II.5) one obtains:

$$\frac{dN}{dE} = \frac{dN}{dt} \cdot \frac{dt}{dE} = \sigma(E/A)\ v\ n_o\ N(E) \cdot \frac{t_s}{2E} \cdot \frac{1}{1 + (E_c/E)^{3/2}}$$

With eq. (II.2), $v = 1.39 * 10^6 * (E/A)^{1/2}$ cm/s (E in eV), Z = 1 and $\ln\Lambda = 15$ it follows:

$$\frac{dN}{dE} = 2.91 * 10^{13}\ A^{1/2}\ \frac{n_o}{n_e}\ \frac{E \cdot \sigma(E/A)}{(E_c/T_e)^{3/2} + (E/T_e)^{3/2}}\ N(E) \qquad \text{(III.1)}$$

Integration from E_o to E with $\gamma = 2.91 * 10^{13}$ results in:

$$N(E) = N_o \exp\left\{ - \gamma A^{1/2}\ \frac{n_o}{n_e} \int_E^{E_o} \frac{E' \cdot \sigma(E'/A)\ dE'}{(E_c/T_e)^{3/2} + (E'/T_e)^{3/2}} \right\} \qquad \text{(III.2)}$$

The decrease of fast ion number with decreasing energy is, therefore, given by (eq. (III.2) in eq. (III.1):

$$\frac{dN(E)}{dE} = \gamma A^{1/2} \frac{n_o}{n_e} \frac{E\,\sigma(E/A)}{(E_c/T_e)^{3/2}+(E/T_e)^{3/2}} \cdot N_o \exp\{-\gamma A^{1/2} \frac{n_o}{n_e} \int_E^{E_o} \frac{E'\,\sigma(E'/A)\,dE'}{(E_c/T_e)^{3/2}+(E'/T_e)^{3/2}}\} \qquad (III.3)$$

The relative particle losses due to CX after slowing-down to the thermal ion temperature T_i can be defined as $L_p = (N_o - N(T_i))/N_o$. One obtains:

$$L_p = 1 - \exp\{-\gamma A^{1/2} \frac{n_o}{n_e} \int_{T_i}^{E_o} \frac{E\,\sigma(E/A)\cdot dE}{(E_c/T_e)^{3/2} + (E/T_e)^{3/2}}\} \qquad (III.4)$$

Here, it is assumed that the equations for the slowing-down velocity (II.4) and for the particle loss-rate (II.5) are valid for all energies down to the ion temperature. However, as long as $E_o >> T_i$, the result of eq. (III.4) is hardly sensitive to the choice of the lower intergration limit T_i; the possible violation of these assumptions, therefore, does not play a significant role.

Figure 2 and figures 12 - 17 show the behaviour of $L_p = f(n_o/n_e)$ for several T_e- and E_o-values, supposing H^o-injection into a hydrogen plasma ($A = A_f = 1$). In all cases $T_i = 1$ keV has been used for the sake of simplicity. Estimations of neutral background densities in existing tokamaks have yielded n_o-values of some 10^8 cm^{-3} /1, 4/, leading to (n_o/n_e)-values in the 10^{-5} range, provided that the plasma densities involved are not too high. In this range, however, the curves in Fig. 2 are strongly increasing. Particle losses and the effects associated with them (energy losses, impurity influx), therefore, may not be neglected.

The results obtained for H^o-injection into a hydrogen plasma (e.g. Fig. 2) can also be applied to cases, where arbitrary hydrogen isotopes are injected into a plasma consisting (predominantly) of

hydrogen isotopes, i.e. to cases where $A \neq 1$ and/or $A_i \neq 1$. In order to do this, an appropriate re-interpretation of the parameters (n_o/n_e), T_e, E_o and T_i must be performed. For H^o-injection into a hydrogen plasma eq. (III.4) reduces to (A, $A_i = 1$):

$$L_p = 1 - \exp\left\{- \frac{\gamma}{(14{,}8)^{3/2}} \cdot \left(\frac{n_o}{n_e}\right)_H \cdot \frac{1}{[Z]_H} \int_{T_{iH}}^{E_{oH}} \frac{E\,\sigma(E)\,dE}{1 + \left(\frac{E}{14.8T_{eH}}\right)^{3/2} \frac{1}{[Z]_H}}\right\} \quad \text{(III.5)}$$

In the general case (A, $A_i \neq 1$) eq. (III.4) is identical to ($\eta = E/A$):

$$L_p = 1 - \exp\left\{\frac{-\gamma}{(14.8)^{3/2}} \cdot \frac{n_o}{n_e} \cdot A \frac{A_i}{[Z]} \int_{T_{i/A}}^{E_o/A} \frac{\eta\,\sigma(\eta)\,d\eta}{1 + \left(\frac{\eta}{14.8T_e}\right)^{3/2} \cdot \frac{A_i}{[Z]}}\right\} \quad \text{(III.6)}$$

Obviously, eq. (III.6) follows from (III.5) by replacing:

$$\left(\frac{n_o}{n_e}\right)_H = \frac{n_o}{n_e} \cdot A \cdot A_i \frac{[Z]_H}{[Z]}$$

$$T_{eH} = T_e \left\{\frac{1}{A_i} \cdot \frac{[Z]}{[Z]_H}\right\}^{2/3} \quad \text{(III.7)}$$

$$E_{oH} = (E_o/A); \quad T_{iH} = (T_i/A)$$

The results of Fig. 2 may be transferred to any combination of $A \neq 1$ and/or $A_i \neq 1$ by changing the abscissa and the curve parameters according to eqs. (III.7). These transformations are valid also if the plasma consists of a mixture of two or three hydrogen isotopes. Provided that only one isotope is dominant, then $[Z] \tilde{-} [Z]_H \tilde{-} 1$. If we consider for example deuterium injection into a deuterium plasma, the particle losses are equal to those of H^o-injection into a hydrogen plasma if the following relations are fulfilled:

$(n_o/n_e)_D = 0.25*(n_o/n_e)_H$, $T_{eD} = 2^{2/3}*T_{eH}$, $E_{oD} = 2*E_{oH}$ and $T_{iD} = 2*T_{iH}$. For $E_o >> T_i$, the T_i-dependence may be neglected. It is interesting to note that the neutral density must be reduced by a factor of 4 in order to obtain the same particle losses.

III.2 Energy Losses

The variation of the total energy ($W(E) = N(E)*dE$) of the fast ions, passing the energy interval dE, is due to 1) energy transfer to the background plasma (dW_{pl}) and to 2) energy losses (dW_L) connected with the particle losses, described before:

$$dW(E) = dW_{pl}(E) + dW_L(E) = N(E)dE + E\frac{dN(E)}{dE} \cdot dE \qquad \text{(III.8)}$$

The energy loss after slowing-down from E_o to E is obtained by:

$$W_L(E) = -\int_{E_o}^{E} dW_L = \int_{E}^{E_o} E' \frac{dN(E')}{dE'} dE'$$

With eq. (III.3) follows:

$$W_L(E) = \gamma A^{1/2} N_o \frac{n_o}{n_e} \int_{E}^{E_o} \frac{E'^2 \sigma(E'/A)}{(\frac{E_c}{T_e})^{3/2} + (\frac{E'}{T_e})^{3/2}} *$$

$$* \exp\{-\gamma A^{1/2} \frac{n_o}{n_e} \int_{E'}^{E_o} \frac{e \sigma(e/A) de}{(\frac{E_c}{T_e})^{3/2} + (\frac{e}{T_e})^{3/2}}\} dE'$$

The relative energy losses of the fast ions caused by CX-processes during slowing-down may be defined by: $L_W = (W_L(T_i)/W(E_o) = (W_L(T_i)/(N_o*E_o))$:

$$L_W = \frac{\gamma A^{1/2}}{E_o} \cdot \frac{n_o}{n_e} \int_{T_i}^{E_o} \frac{E^2 \, \sigma(E/A)}{(E_c/T_e)^{3/2}+(E/T_e)^{3/2}} \cdot$$

$$\cdot \exp\left\{-\gamma A^{1/2} \frac{n_o}{n_e} \int_{E}^{E_o} \frac{E' \sigma(E'/A) \cdot dE'}{(E_c/T_e)^{3/2}+(E'/T_e)^{3/2}}\right\} dE \qquad \text{(III.9)}$$

Figure 3 and figures 12 - 17 show some graphs for $L_W = f(n_o/n_e)$ based on the assumptions ($A = A_i = 1$) and the parameters corresponding to those of Fig. 2. Note that the relative energy losses for $E_o = 60$ keV are (partly) less than those for $E_o = 20$ keV. This is due to the fact that the slowing-down velocity strongly decreases with decreasing energy provided that $E \gtrsim 20$ keV(Fig. 1). The highly energetic ions, therefore, are predominantly lost after giving up most of their energy to the plasma particles.

Again, the results obtained for H^o-injection into a hydrogen plasma (e.g. Fig. 3) may be transferred to cases of arbitrary A- and A_i-values (Z = 1) by applying the transformations (III.7).

III.3 Impurity Influx

The fast CX-neutrals which escape from the plasma represent a source of impurity influx to the plasma, since they produce heavy impurity atoms by sputtering processes on the walls. An upper limit for this influx will be obtained by assuming that all fast CX-neutrals hit the walls and, furthermore, all sputtered atoms reach the plasma. Due to the finite slowing-down time the onset of the impurity influx is delayed compared to the beginning of the neutral beam. Provided constant neutral beam intensity, the influx of heavy atoms will be

proportional to the injected neutral current after, approximately, one slowing-down time τ_o. The following considerations are valid for such steady state conditions.

The number of neutrals created within the energy interval (E, E-dE) is given by:

$$dN_n(E) = - dN(E) = - \frac{dN(E)}{dE} \cdot dE$$

Using eq. (III.3) and defining:

$$F(E) \equiv \gamma A^{1/2} \frac{n_o}{n_e} \cdot \frac{E \cdot \sigma(E/A)}{(E_c/T_e)^{3/2} + (E/T_e)^{3/2}} *$$

$$* \exp\{ -\gamma A^{1/2} \frac{n_o}{n_e} \int_E^{E_o} \frac{E' \cdot \sigma(E'/A) \cdot dE'}{(\frac{E_c}{T_e})^{3/2} + (\frac{E'}{T_e})^{3/2}} \}$$

one obtains:

$$dN_n = - N_o \cdot F(E)\, dE \qquad \text{(III.10)}$$

In order to describe the impurity influx in the picture of particle currents, it will be introduced as an additional assumption that the neutral particle current (I_o/e), which is absorbed and confined within the plasma, is constant during the beam pulse ($\tau_{pul.}$). From the definition of N_o it follows:

$$N_o = (I_o/e)\tau_{pul} \qquad \text{(III.11)}$$

The particle current of CX-neutrals with energy E escaping from the plasma is then given by:

$$dI_n = - \frac{dN_n}{\tau_{pul.}} = - (I_o/e) \cdot F(E) \cdot dE$$

This current causes an influx of sputtered atoms:

$$dI_s = S(E) \cdot dI_n = - (I_o/e) \cdot S(E) \cdot F(E)\, dE$$

where S(E) denotes the sputtering coefficient at energy E. The total impurity influx into the plasma is, obviously, obtained by integrating over energy from E_o to T_i:

$$I_s = (I_o/e) \int_{T_i}^{E_o} S(E)\, F(E)\, dE \qquad \text{(III.12)}$$

or

$$I_s = (I_o/e)\, \gamma \cdot A^{1/2} \frac{n_o}{n_e} \int_{T_i}^{E_o} \frac{S(E)\,\sigma(E/A)E}{(\frac{E_c}{T_e})^{3/2} + (\frac{E}{T_e})^{3/2}} \cdot$$

$$\cdot \exp\left\{-\gamma A^{1/2} \frac{n_o}{n_e} \int_{E}^{E_o} \frac{E'\sigma(E'/A)\, dE'}{(\frac{E_c}{T_e})^{3/2} + (\frac{E'}{T_e})^{3/2}}\right\} dE$$

In calculating the curves illustrated in Fig. 4, the sputtering coefficient for H^+ on stainless steel, summarized by Scherzer /5/, were used. The further assumptions ($A = A_i = 1$) and parameters correspond to those of Figs. 2 and 3.

The behaviour of I_s, especially the decrease at higher (n_o/n_e)-values may be explained from the energy dependence of the sputtering

coefficients. For $E \gtrsim 3$ keV the sputtering yield is a decreasing function of incident particle energy.

The results in Fig. 4 may, evidently, not be applied to other hydrogen isotopes, since the sputtering yield strongly depends on the incident particle species. It should be mentioned, however, that the impurity influx will increase if deuterium or tritium beams are injected due to the higher sputting coefficients for these isotopes /5/.

IV. CHARGE EXCHANGE LOSSES AND IMPURITY INFLUX FOR GIVEN PROFILES

The results of the preceding section have shown that the particle losses and, therefore, the associated energy losses and the impurity influx strongly depends on (n_o/n_e) and T_e. In all experimental devices these parameters exhibit a considerable variation over the plasma cross-section (e.g. ORMAK: $n_o(a) \simeq 20\ n_o(0)$ /4/). In addition, the initial fast ion density created by neutral injection is a function of the minor radius r. This calls for the allowance of (n_o/n_e)- and T_e-profiles as well as for fast ion deposition profiles in the calculational formalism, outlined above. This will be done by, first, calculating the local losses; radial integration subsequently determines the total particle losses, energy losses and the resulting impurity influx.

The radial distribution of the fast ion input rate due to neutral injection can be written according to Rome et al. /4/ as:

$$\dot{n}_f(r) = \frac{(I_o/e)}{2\pi R_o \pi a^2}\ H(r) \qquad \text{(IV.1)}$$

where H(r) is a (dimensionless) shape factor, further called "deposition profile", which is determined by injection geometry, injection energy, plasma parameters and beam trapping cross sections. H(r) is normalized in such a way, that:

$$F \equiv \frac{1}{V_{pl}} \int_{V_{pl}} H(r)dV = \frac{2}{a^2} \int_0^a H(r)\, r\, dr \qquad \text{(IV.2)}$$

($V_{pl} = 2\pi R \pi a^2$). F denotes the relative amount of the injected beam which is absorbed and confined within the plasma. For the following it is assumed that the fast ions are sticked to their drift surfaces during slowing-down, i.e. H(r) will not be changed by collisional energy transfer. This may be justified for tangential injection where the ions describe passing orbits, far away from trapping into the toroidal mirrors.

The radial dependence of the number of fast particles created during one neutral beam pulse,assuming constant beam intensity and beam energy E_o, is given by:

$$N_o(r) = (I_o/e)\, \tau_{pul}\, H(r) \qquad \text{(IV.3)}$$

After slowing-down to energy E the number of remaining particles can be calculated using eqs. (III.2) and (IV.3):

$$N(E,r) = (I_o/e)\tau_{pul}\, H(r)\, \exp\left\{-\gamma A^{1/2} \frac{n_o}{n_e} \int_E^{E_o} \frac{E'\, \sigma(\frac{E'}{A})\, dE'}{(\frac{E_c}{T_e})^{3/2} + (\frac{E'}{T_e})^{3/2}}\right\} \qquad \text{(IV.4)}$$

The volume integrated relative particle losses after fast ion thermalization will be obtained according to the following definition:

$$L_{p,v} \equiv \int_{V_{pl}} \frac{N_o(r) - N(T_i, r)}{N_o(r)} \, dV$$

With eq. (IV.4) follows:

$$L_{p,v} = \frac{2}{a^2} \int_o^a H(r) \left[1 - \exp\left\{ -\gamma A^{1/2} \frac{n_o}{n_e}(r) \int_{T_i}^{E_o} \frac{E\,\sigma(E/A)\,dE}{\left(\frac{E_c(r)}{T_e(r)}\right)^{3/2} + \left(\frac{E}{T_e(r)}\right)^{3/2}} \right\} \right] r \, dr \quad \text{(IV.5)}$$

or

$$L_{p,v} = \frac{2}{a^2} \int_o^a H(r)\, L_p(r)\, r \, dr$$

$L_p(r)$ is defined by eq. (III.4) where (n_o/n_e), T_e and E_c should be taken at the location r. The radial dependence of T_i is neglected since the result of (IV.5) is not sensitive to T_i, provided that $T_i \ll E_o$. According to the normalization of H(r), the relative particle losses are related to the number of neutrals hitting the plasma surface (not to the number of neutrals absorbed and confined within the plasma).

Eqs. (III.9) and (III.12) for the relative energy losses and the impurity influx, respectively, may be extended in an analoguous way. Again, the resulting terms are related to the energy and current, respectively, injected into the torus. One obtains:

$$L_{W,r} = \frac{2}{a^2} \int_o^a H(r)\, L_W(r)\, r \, dr \quad \text{(IV.6)}$$

$$I_{s,v} = \frac{2}{a^2} \int_o^a H(r)\, I_s(r)\, r \, dr \quad \text{(IV.7)}$$

Here, $L_W(r)$ and $I_s(r)$ are defined by eqs. (III.9) and (III.12) taking the local values of (n_o/n_e), T_e, and E_c.

In the following some results of eqs. (IV.5), (IV.6) and (IV.7) will be illustrated. They are taken from calculations being performed for the planned injection experiment on ASDEX. H^o-injection into a hydrogen plasma has been assumed. The applied profiles (n_o/n_e) (r), $T_e(r)$ and H(r) are displayed in Fig. 5. (For further information concerning these profiles, see ref. /6/). Results for $L_{p,v}$, $L_{W,v}$ and $(I_{s,v}/I_o)$ are plotted in Figs. 6-8. The decreasing values of the relative energy losses for $E_o \gtrsim 40$ keV result again from increasing slowing-down velocity and decreasing CX-cross section at high energy; CX probability, therefore, will become smaller.

V. ENERGY TRANSFER TO PLASMA IONS AND ELECTRONS

V.1 Constant Plasma Parameters

The energy transfer from the fast ions to the background plasma will be investigated in order to obtain the local and integral fraction of the injected energy given up to the ions and electrons, respectively, including the CX-losses. The calculations are similar to those of Callen et al./7/, the complete energy dependence of the CX-cross section (II.6), however, will be taken into account.

According to eq. (III.8), the variation of fast ion energy due to slowing-down collisions with the background plasma is given by:

$$dW_{pl}(E) = N(E)dE = N(E)\,(f_I(E) + f_e(E))\,dE$$

Here, $f_I(E)$ and $f_e(E)$ denote the relative differential energy division into plasma ions and electrons, respectively

($f_I(E) + f_e(E) = 1$). Using the formalism described by Stix /2/ one obtains:

$$f_I(E) = \{1 + (E/E_c)^{3/2}\}^{-1}$$
$$f_e(E) = \{1 + (E_c/E)^{3/2}\}^{-1} \qquad (V.1)$$

The variation of the plasma particle energy due to fast ion deceleration from E to E - dE can then be written:

$$dW_I(E) = - N(E)\, f_I(E)\, dE = - \frac{N(E)\, dE}{1 + (E/E_c)^{3/2}}$$

$$dW_e(E) = - N(E)\, f_e(E)\, dE = - \frac{N(E)\, dE}{1 + (E_c/E)^{3/2}}$$

Introducing eq. (III.2) and subsequent integration yield:

$$W_I(E) = N_o \int_E^{E_o} \frac{1}{1+(\frac{E'}{E_c})^{3/2}} \exp\{-\gamma A^{1/2} \frac{n_o}{n_e} \int_{E'}^{E_o} \frac{e\,\sigma(e/A)de}{(\frac{E_c}{T_e})^{3/2}+(\frac{e}{T_e})^{3/2}}\}\, dE'$$

$$W_e(E) = N_o \int_E^{E_o} \frac{1}{1+(\frac{E_c}{E'})^{3/2}} \exp\{-\gamma A^{1/2} \frac{n_o}{n_e} \int_{E'}^{E_o} \frac{e\,\sigma(e/a)\,de}{(\frac{E_c}{T_e})^{3/2}+(\frac{e}{T_e})^{3/2}}\}\, dE' \qquad (V.2)$$

After slowing-down to thermal energies T_i, the fraction of initial beam energy, given up to ions and electrons, respectively, is determined by:

$$G_I \equiv \frac{W_I(T_i)}{N_o E_o} = \frac{1}{E_o} \int_{T_i}^{E_o} \frac{1}{1+(\frac{E}{E_c})^{3/2}} \exp\{-\gamma A^{1/2} \frac{n_o}{n_e} \int_E^{E_o} \frac{E'\sigma(\frac{E'}{A})dE'}{(\frac{E_c}{T_e})^{3/2}+(\frac{E'}{T_e})^{3/2}}\}dE$$

$$G_e \equiv \frac{W_e(T_i)}{N_o E_o} = \frac{1}{E_o} \int_{T_i}^{E_o} \frac{1}{1+(\frac{E_c}{E})^{3/2}} \exp\{-\gamma A^{1/2} \frac{n_o}{n_e} \int_E^{E_o} \frac{E'\sigma(\frac{E'}{A})dE'}{(\frac{E_c}{T_e})^{3/2}+(\frac{E'}{T_e})^{3/2}}\}dE \qquad (V.3)$$

By neglecting CX-losses ($n_o = 0$), formulae (V.3) become identical with the results of Stix /2/. In Fig. 9, graphs of G_I and G_e as function of (E_o/E_c) are shown for several (n_o/n_e)-values. The calculations were done assuming H^o-injection into a hydrogen plasma. Figure 9 indicates that, in particular, the ion heating is affected by the CX-losses. Using the transformations (III.7), the G_I- and G_e-graphs can be applied again to cases where A and/or $A_i \neq 1$.

V.2 Determination of Heating Power Profiles

In order to introduce fast ion deposition profiles H(r) as well as a radial dependence of (n_o/n_e), T_e and E_c, the formalism of section V.1 has to be extended in a way similar to that, outlined in chapter IV.

The total neutral beam energy injected into the torus during one beam pulse is given by:

$$E_{in} = (I_o/e)\ \tau_{pul}\ E_o = I_o\ U_o\ \tau_{pul} \qquad (V.4)$$

Again, (I_o/e) stands for the neutral particle current hitting the plasma surface. The relative fraction of E_{in} transferred to the plasma ions after slowing-down is:

$$R_I = \frac{1}{E_{in} \cdot V_{pl}} \int_{V_{pl}} W_I(T_i,r)\ dV$$

Here, $W_I(T_i,r)$ is defined by eq. (V.2) with the local values of $N_o(r)$, $(n_o/n_e)\ (r)$, $T_e(r)$ and $E_c(r)$; $N_o(r)$ is given by eq. (IV.3). Using eq. (V.4) one obtains:

$$R_I = \frac{2}{a^2} \int_0^a H(r)\, G_I(r)\, r\, dr$$

and

$$R_e = \frac{2}{a^2} \int_0^a H(r)\, G_e(r)\, r\, dr \qquad (V.5)$$

$G_I(r)$ and $G_e(r)$ are the local, energy integrated fractions of the injected beam energy given up to the ions and electrons, respectively, as defined in eqs. (V.3). The total balance of the neutral beam energy is, therefore, given by:

$$E_{in} = (L_{W,v} + R_I + R_e)\, E_{in} + (1\text{-}F)\, E_{in}$$

The term E_{in} (1-F) denotes, according to the definition of F (eq.(IV.2)), the neutral beam fraction not absorbed or confined within the plasma.

The heating power transferred to the ions and electrons can be written as:

$$P_I = \frac{2\, I_o U_o}{a^2} \int_0^a H(r)\; G_I(r)\, r\, dr$$

$$P_e = \frac{2\, I_o U_o}{a^2} \int_0^a H(r)\; G_e(r)\, r\, dr \qquad (V.6)$$

and for the local heating power density, therefore, follows:

$$p_I(r) = \frac{I_o U_o}{V_{pl}} \cdot H(r)\; G_I(r)$$

$$p_e(r) = \frac{I_o U_o}{V_{pl}}\, H(r)\, G_e(r) \qquad (V.7)$$

The knowledge of local heating power density is necessary if it is intended to control plasma profiles (e.g. $T_e(r)$, $T_i(r)$, $j(r)$) by depositing the injected power in a definite manner ("profile-shaping"). Some examples for $p_I(r)$ and $p_e(r)$, calculated for ASDEX dimensions, are illustrated in Fig.10. The different graphs were obtained by changing the injection geometry. The curve parameters specify the minimum distance between beam axis and torus symmetry axis.

The various deposition profiles involved in the calculations are reported elsewhere /8/. The local heating power densities for the ions (Fig. 11) are different from those for the electrons, especially in the outer plasma regions. Here the increasing neutral background density reduces the ion heating.

VI. CONCLUDING REMARKS

The calculations, outlined above, have been performed in the framework of the preparations of the planned injection experiments on W VIIa and ASDEX. They should allow to estimate the particle losses, energy losses and the impurity influx which will be expected due to CX-processes during fast particle slowing-down and to determine the heating power transferred to the plasma particles. More detailed applications will be found in ref. /6/.

A complete treatment of the particle slowing-down process, however, calls for taking into account pitch-angle scattering and the associated loss-region in velocity space /9/. Furthermore, the outlined formalism

implicitly assumes that the plasma parameters ($T_e(r)$, $n_e(r)$ or $n_o(r)$) does not significantly vary during the neutral beam pulse. In order to include such variations, a self-consistent coupling of the above calculations to an appropriate plasma simulation code has to be performed.

The authors wish to acknowledge many valuable discussions with Dr. J.H. Feist.

REFERENCES

/1/ TFR-Group, 3rd Intern. Meeting on Theoret. and Experim. Aspects of Heating of Toroidal Plasmas, Grenoble 1976, Vol. 2, p. 141.

/2/ T.H. Stix, Plasma Physics 14 (1971) 367.

/3/ A.C. Riviere, Nuclear Fusion 11 (1971) 363.

/4/ J.A. Rome, J.D. Callen, J.F. Clarke, Nuclear Fusion 14 (1974) 141.

/5/ B.M.U. Scherzer, J. Vac. Sci. Technol. 13 (1976) 420.

/6/ A. Staebler, Lab. Rep. IPP IV/159.

/7/ J.D. Callen et al., 5th Int. Conf. on Plasma Physics and Controlled Nuclear Fusion, Tokyo 1974, Vol. 1, p. 645.

/8/ G. Haas et al., 3rd Symp. on Plasma Heating in Toroidal Devices, Varenna 1976, p. 306.

/9/ J.A. Rome et al., Nuclear Fusion 16 (1976) 55.

FIGURE CAPTIONS

Fig. 1 Slowing-down time (τ_o) and slowing-down velocity ($\frac{dE}{dt}$) of hydrogen ions in a hydrogen plasma vs. ion energy (E_o) with the electron temperature (T_e) as parameter.

Fig. 2 Relative particle loss (L_p) for H^o-injection into a hydrogen plasma vs. ratio of neutral background density to plasma density ($\frac{n_o}{n_e}$) for various energies (E_o) and electron temperatures (T_e).

Fig. 3 Relative energy loss (L_W) for H^o-injection into a hydrogen plasma vs. ratio of neutral background density to plasma density (n_o/n_e) for various energies (E_o) and electron temperatures (T_e).

Fig. 4 Impurity influx (I_{IMP}) induced by injection of 1 A of hydrogen atoms into a hydrogen plasma vs. ratio of neutral background density to plasma density (n_o/n_e) for various energies (E_o) and electron temperatures (T_e).

Fig. 5 Radial profiles of electron temperature (T_e), ratio of neutral background density to plasma density (n_o/n_e) and deposition profile H(r).

Fig. 6 Integrated relative particle loss ($L_{p,v}$) for H^o-injection into a hydrogen plasma vs. injection energy (E_o) for ASDEX plasma parameters of fig. 5.

Fig. 7 Integrated relative energy loss ($L_{W,v}$) for H^0-injection into a hydrogen plasma vs. injection energy (E_0) for ASDEX plasma parameters of fig. 5

Fig. 8 Integrated impurity influx (I_{IMP}) induced by injection of 1 A of hydrogen atoms into a hydrogen plasma vs. injection energy (E_0) for ASDEX plasma parameters of fig. 5.

Fig. 9 Energy transfer from injected hydrogen ions to hydrogen plasma ions (G_I) and electrons (G_e) vs. ratio of injection energy to critical energy (E_0/E_c) for various (n_0/n_e)-ratios.

Fig. 10 Radial electron heating power density profile (P_e) with the minimum distance between beam axis and torus center (R_c) as parameter.

Fig. 11 Radial ion heating power density profile (P_I) with the minimum distance between beam axis and torus center (R_C) as parameter.

Fig. 12, 13, 14, 15 Lines of constant relative particle (L_p) and energy (L_w) losses for H^0-injection into a hydrogen plasma at injection energies of 10, 30, 50, 80 keV.

Fig. 16 10 %-particle (L_p) and energy (L_W) loss curves for H^0-injection into a hydrogen plasma at various injection energies (E_0).

Fig. 17 Relative particle (L_p) and energy (L_w) losses for H^o-injection into a hydrogen plasma vs. injection energy (E_o) for various ratios of neutral background density to plasma density (n_o/n_e) and an electron temperature of T_e = 1 keV.

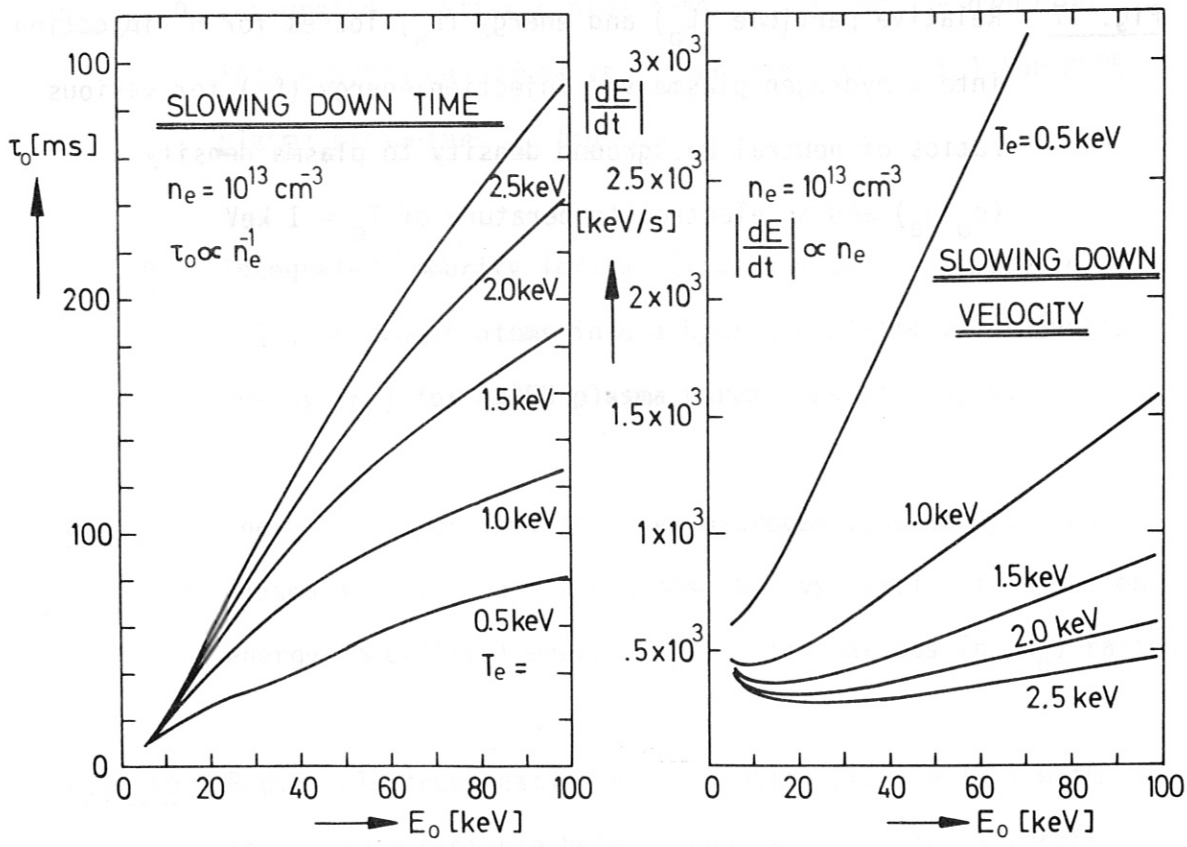
SLOWING DOWN TIME
$n_e = 10^{13}\ cm^{-3}$
$\tau_o \propto n_e^{-1}$
τ_o[ms]
2.5keV
2.0keV
1.5keV
1.0keV
0.5keV
T_e =
E_o [keV]
$\left|\frac{dE}{dt}\right|$ [keV/s]
$n_e = 10^{13}\ cm^{-3}$
$\left|\frac{dE}{dt}\right| \propto n_e$
SLOWING DOWN VELOCITY
T_e=0.5keV
1.0keV
1.5keV
2.0 keV
2.5 keV
E_o [keV]

Fig. 1

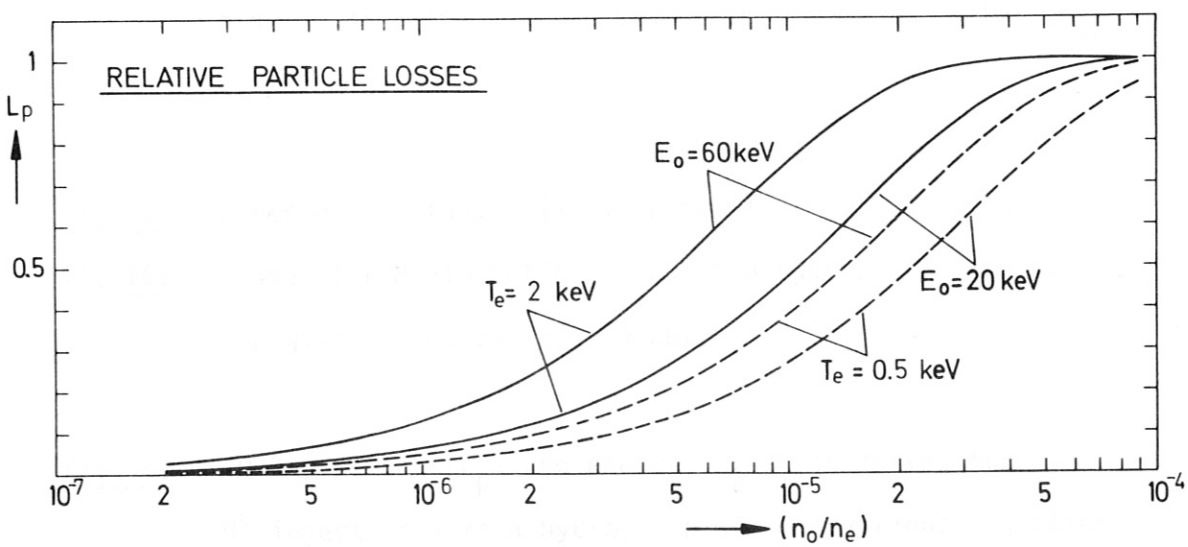
RELATIVE PARTICLE LOSSES
L_p
E_o=60keV
T_e= 2 keV
E_o=20 keV
T_e = 0.5 keV
(n_o/n_e)

Fig. 2

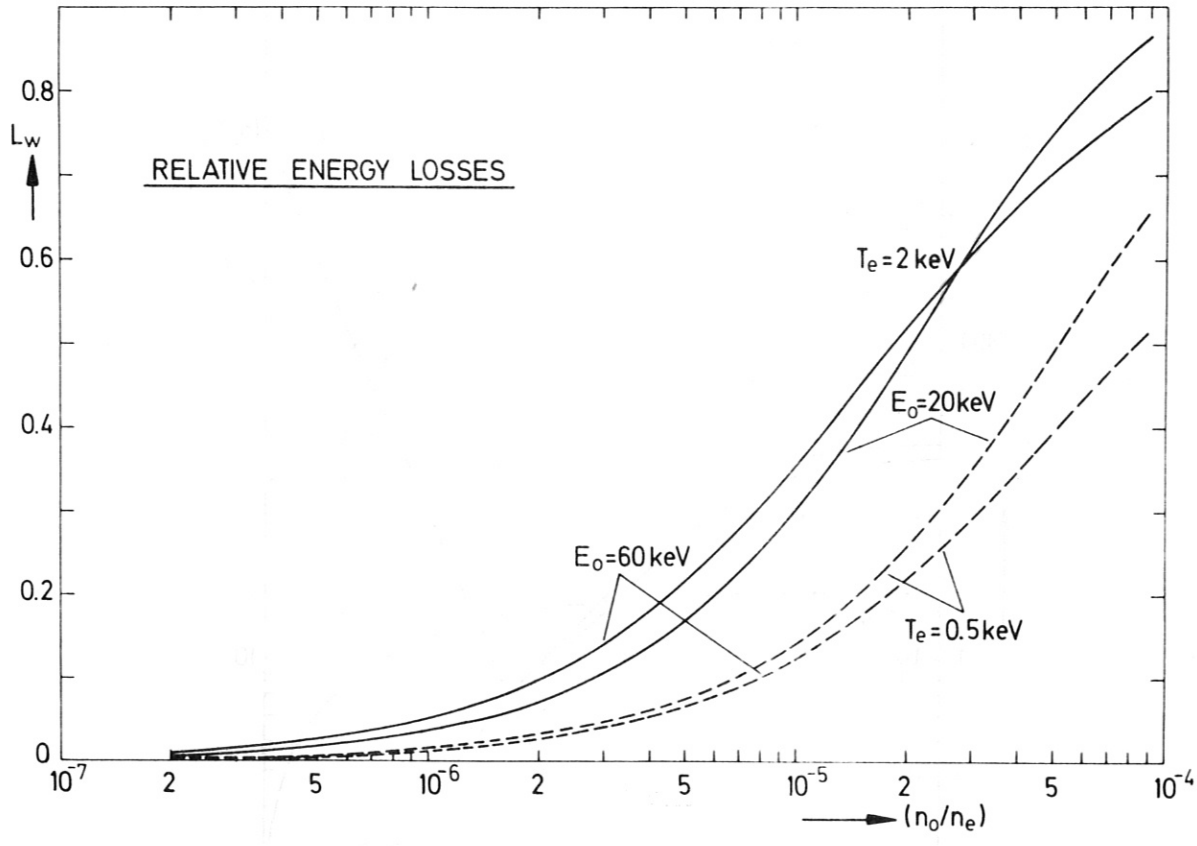
RELATIVE ENERGY LOSSES
L_w
0.8
0.6
0.4
0.2
0
T_e = 2 keV
E_o=20keV
E_o=60keV
T_e = 0.5keV
10^{-7}
2
5
10^{-6}
2
5
10^{-5}
2
5
10^{-4}
(n_o/n_e)

Fig. 3

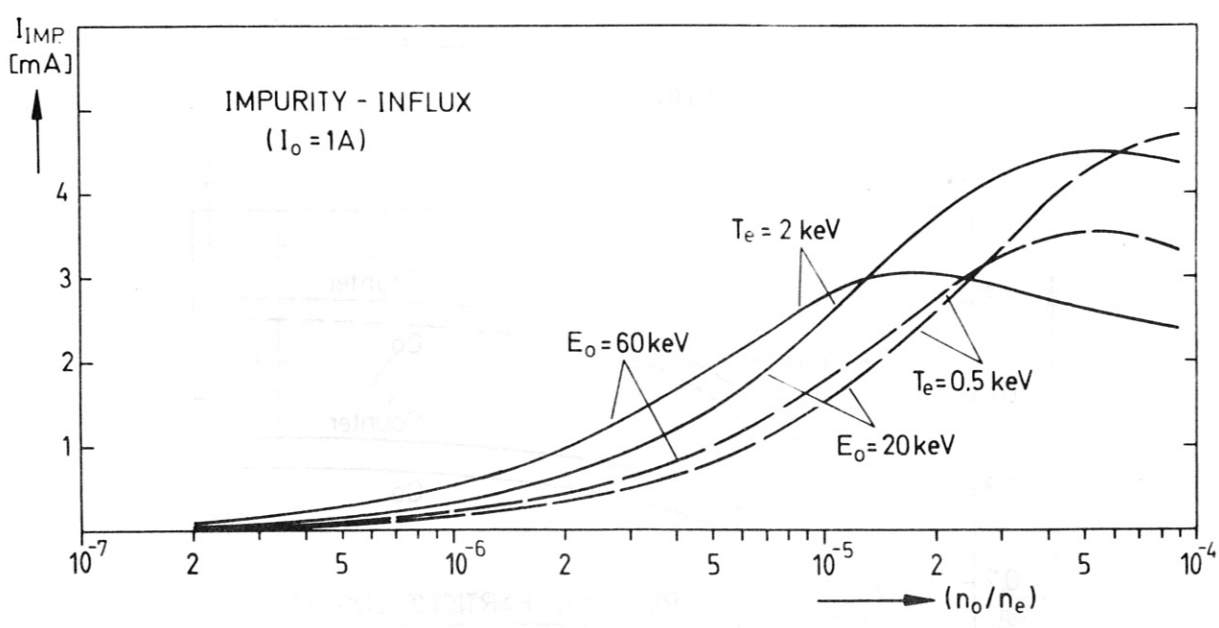
I_{IMP} [mA]
IMPURITY - INFLUX
(I_o = 1A)
4
3
2
1
T_e = 2 keV
E_o = 60keV
T_e = 0.5 keV
E_o = 20keV
10^{-7}
2
5
10^{-6}
2
5
10^{-5}
2
5
10^{-4}
(n_o/n_e)

Fig. 4

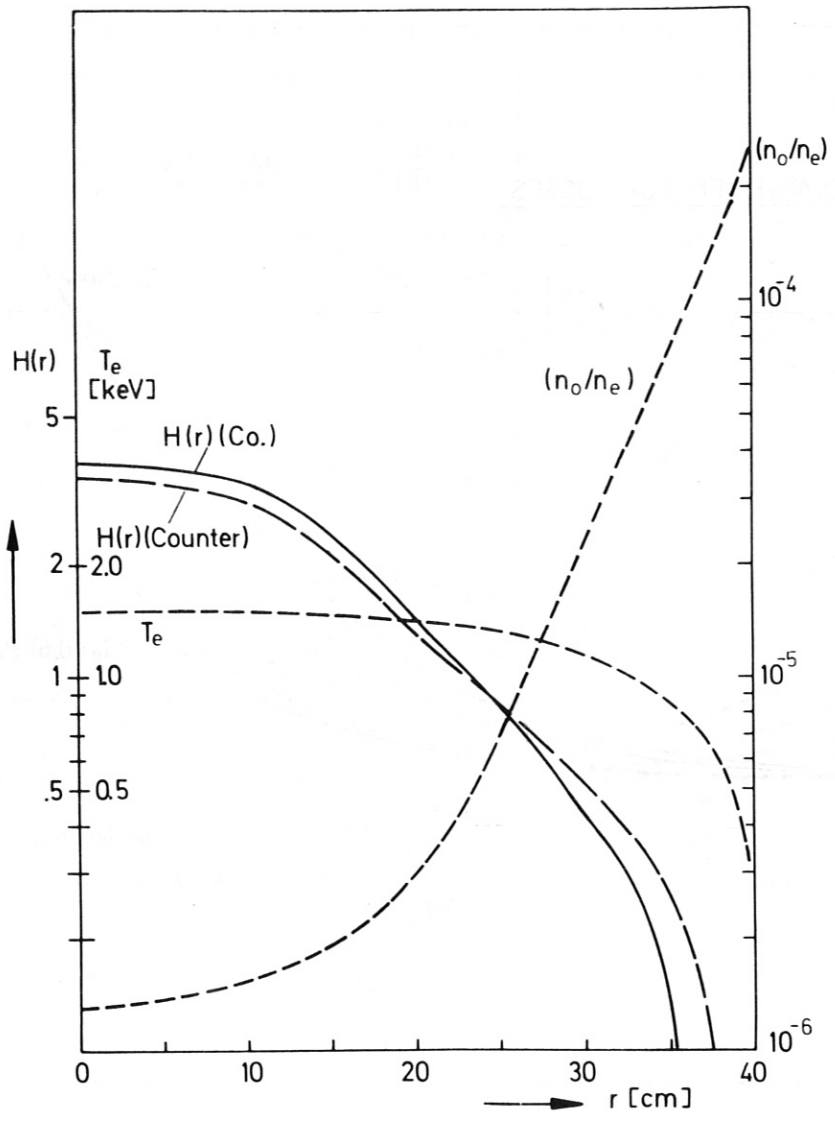
H(r)
T_e [keV]
5
2
2.0
1
1.0
.5
0.5
H(r) (Co.)
H(r)(Counter)
T_e
(n_o/n_e)
(n_o/n_e)
10^{-4}
10^{-5}
10^{-6}
0
10
20
30
40
r [cm]

Fig. 5

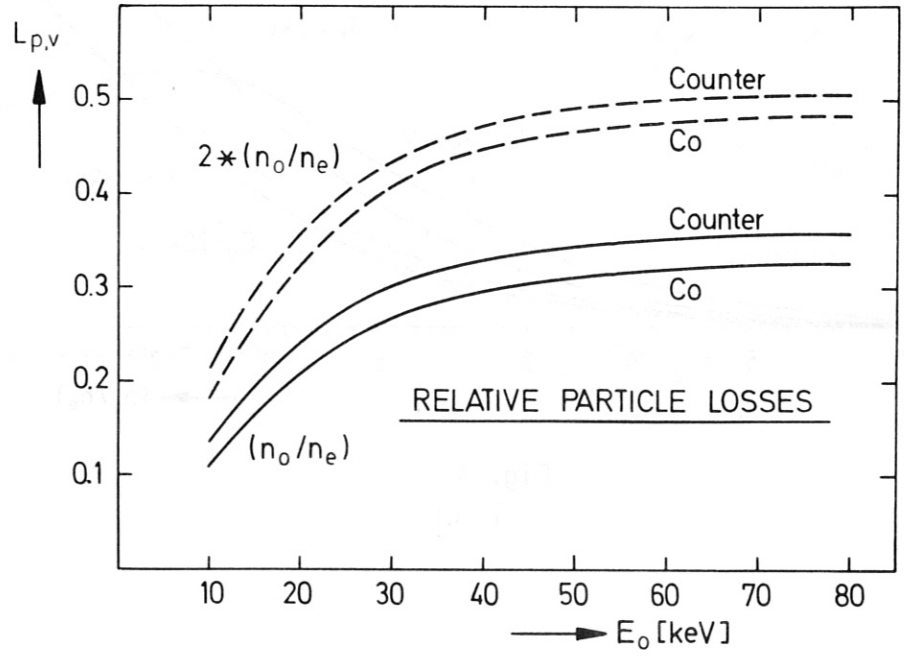
$L_{p,v}$
0.5
0.4
0.3
0.2
0.1
Counter
Co
$2*(n_o/n_e)$
Counter
Co
RELATIVE PARTICLE LOSSES
(n_o/n_e)
10
20
30
40
50
60
70
80
E_o [keV]

Fig. 6

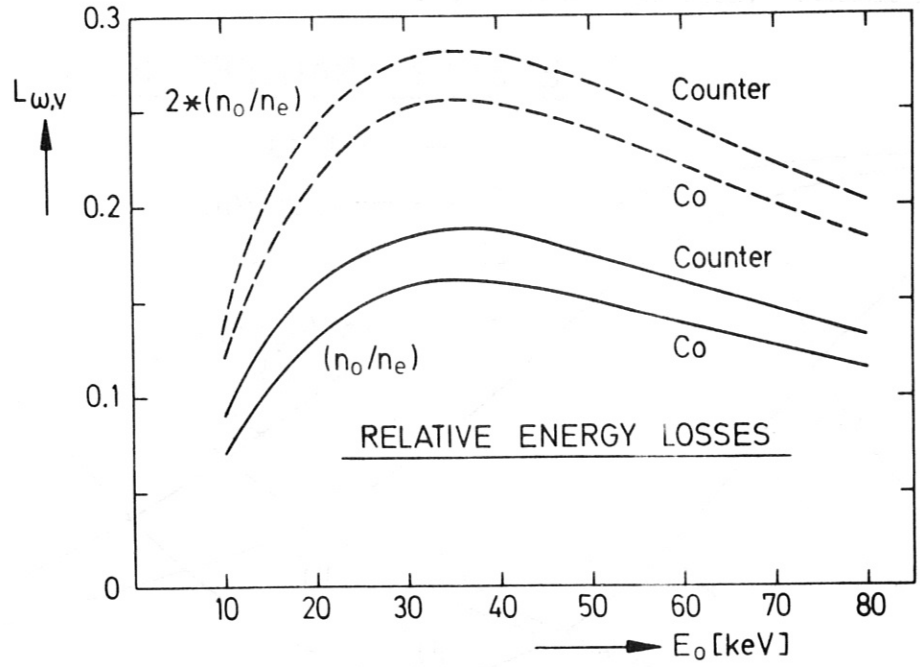
0.3
0.2
0.1
0
$L_{\omega,v}$
$2*(n_o/n_e)$
Counter
Co
Counter
Co
(n_o/n_e)
RELATIVE ENERGY LOSSES
10
20
30
40
50
60
70
80
E_o [keV]

Fig. 7

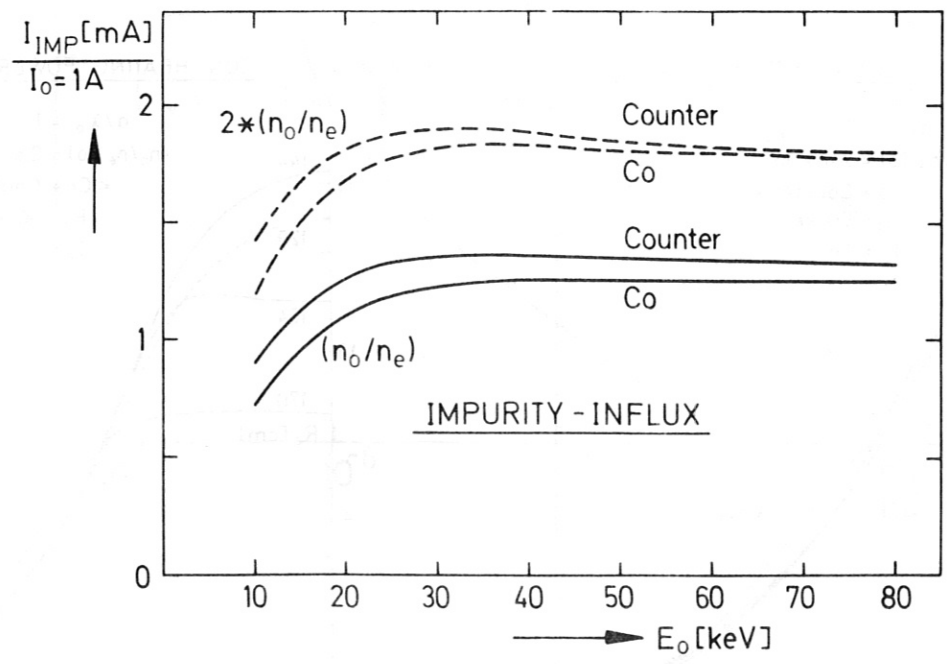
I_{IMP}[mA]
I_o=1A
2
1
0
$2*(n_o/n_e)$
Counter
Co
Counter
Co
(n_o/n_e)
IMPURITY - INFLUX
10
20
30
40
50
60
70
80
E_o [keV]

Fig. 8

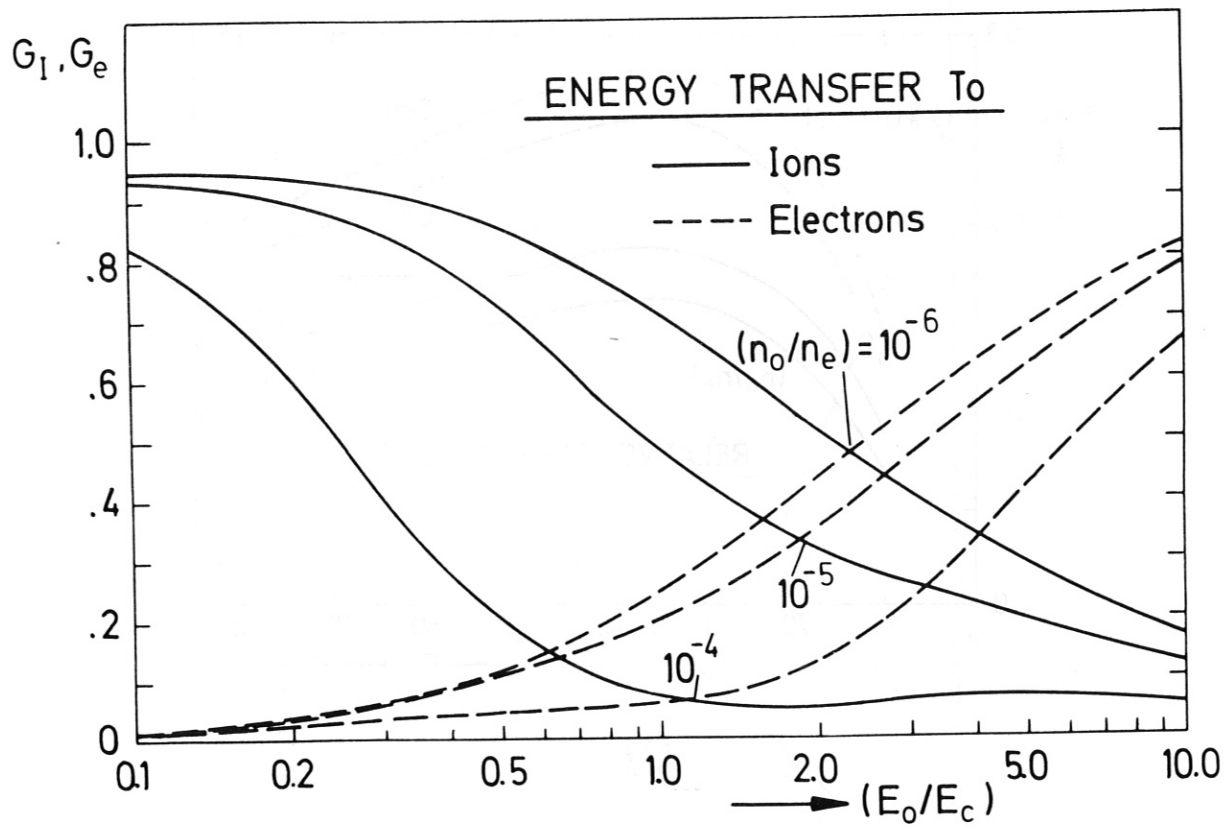

Fig. 9

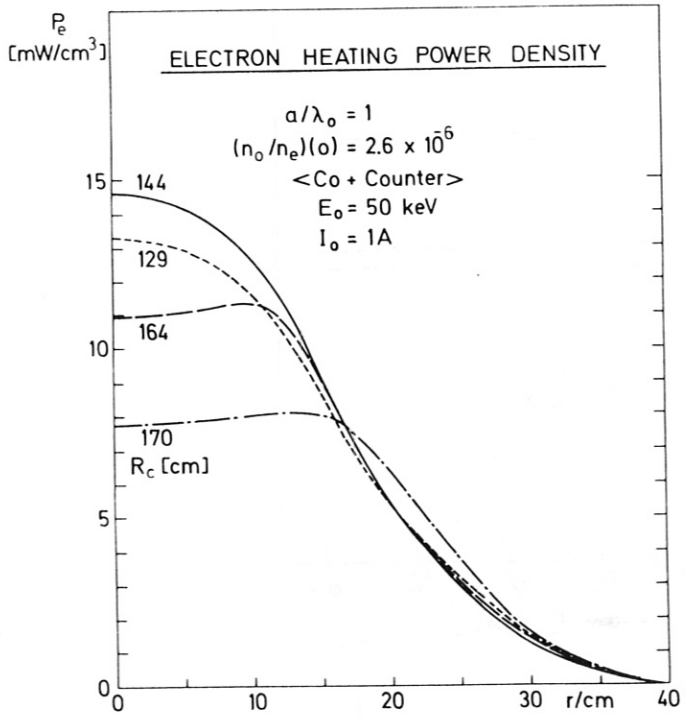

Fig. 10

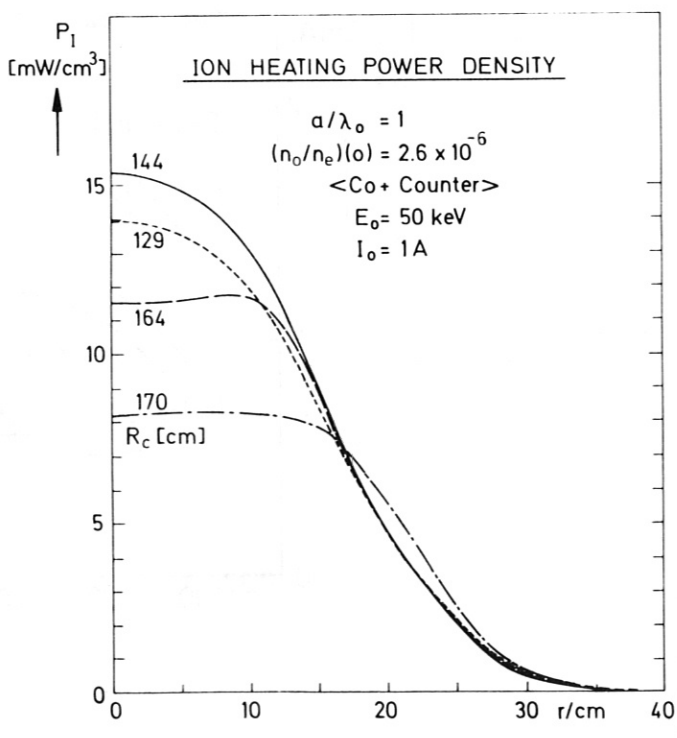

Fig. 11

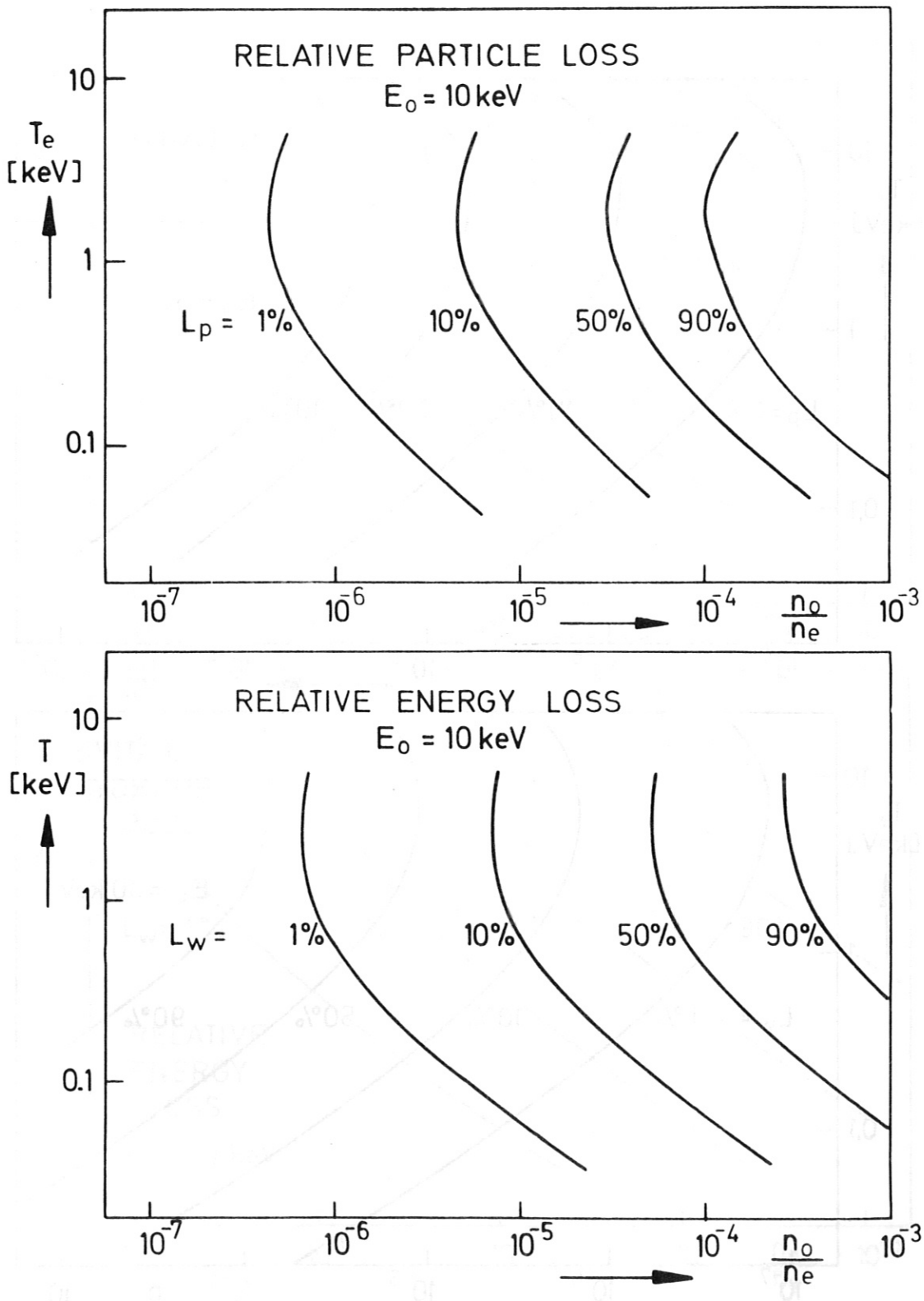
RELATIVE PARTICLE LOSS
E_o = 10 keV
T_e [keV]
10
1
0.1
L_p = 1%
10%
50%
90%
10^{-7}
10^{-6}
10^{-5}
10^{-4}
10^{-3}
$\frac{n_o}{n_e}$
RELATIVE ENERGY LOSS
E_o = 10 keV
T [keV]
10
1
0.1
L_w =
1%
10%
50%
90%
10^{-7}
10^{-6}
10^{-5}
10^{-4}
10^{-3}
$\frac{n_o}{n_e}$

Fig. 12

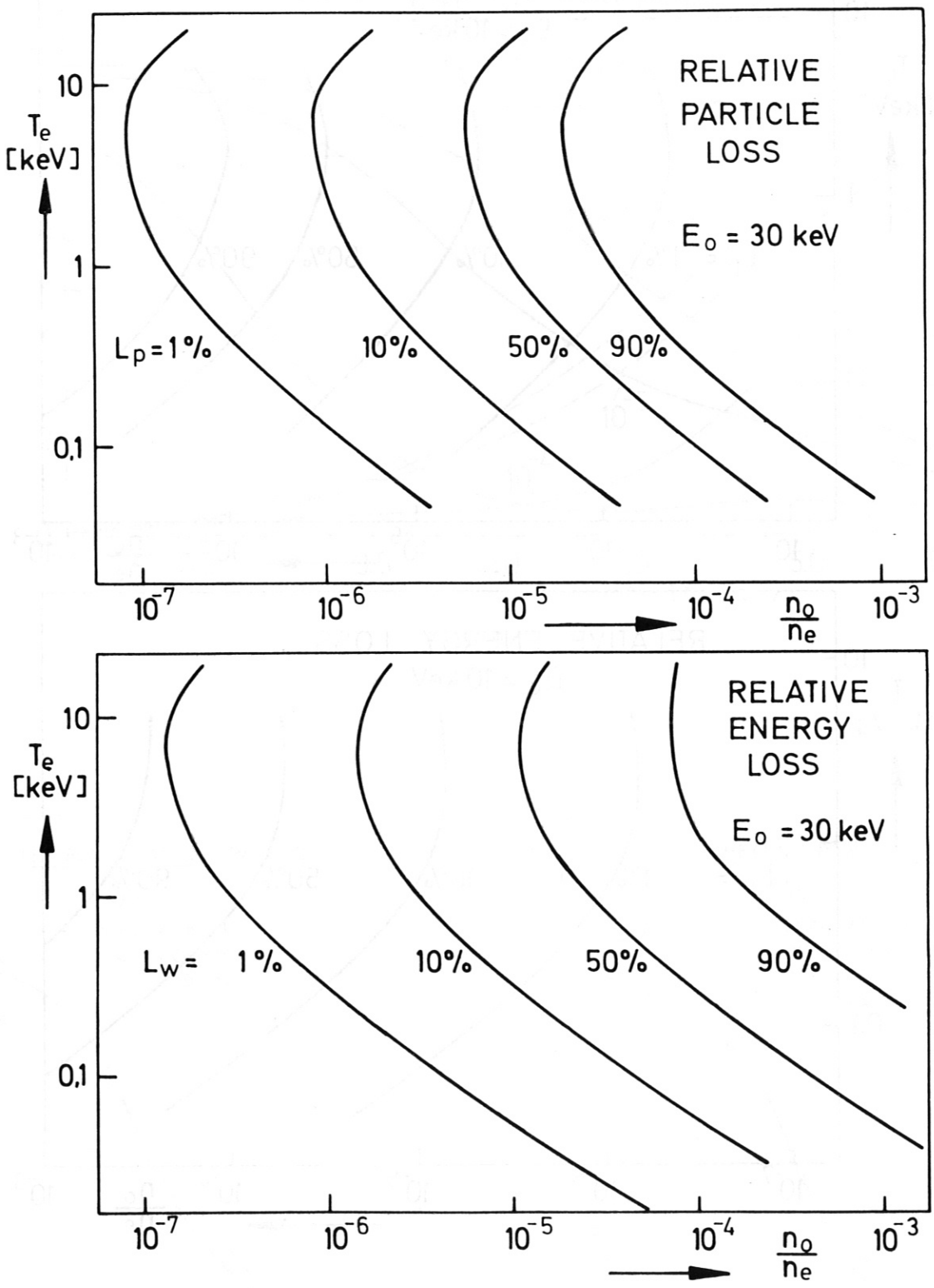
RELATIVE
PARTICLE
LOSS
E_o = 30 keV
L_p = 1 %
10%
50%
90%
T_e [keV]
10
1
0,1
10^{-7}
10^{-6}
10^{-5}
10^{-4}
10^{-3}
$\frac{n_o}{n_e}$
RELATIVE
ENERGY
LOSS
E_o = 30 keV
L_w = 1 %
10%
50%
90%
T_e [keV]
10
1
0,1
10^{-7}
10^{-6}
10^{-5}
10^{-4}
10^{-3}
$\frac{n_o}{n_e}$

Fig. 13

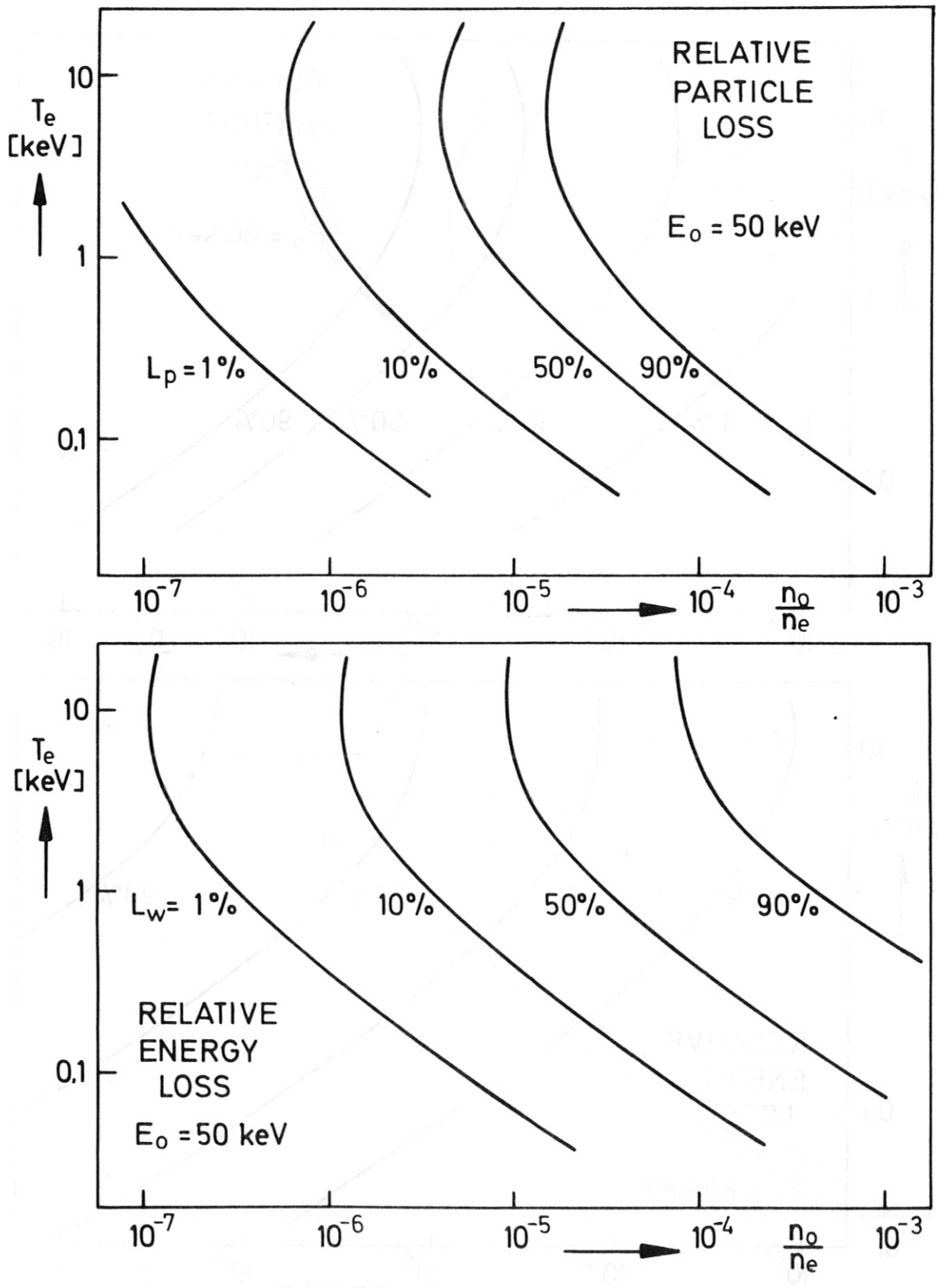
RELATIVE
PARTICLE
LOSS
E_o = 50 keV
T_e [keV]
10
1
0.1
L_p = 1%
10%
50%
90%
10^{-7}
10^{-6}
10^{-5}
10^{-4}
10^{-3}
$\frac{n_o}{n_e}$
T_e [keV]
10
1
0.1
L_w = 1%
10%
50%
90%
RELATIVE
ENERGY
LOSS
E_o = 50 keV
10^{-7}
10^{-6}
10^{-5}
10^{-4}
10^{-3}
$\frac{n_o}{n_e}$

Fig. 14

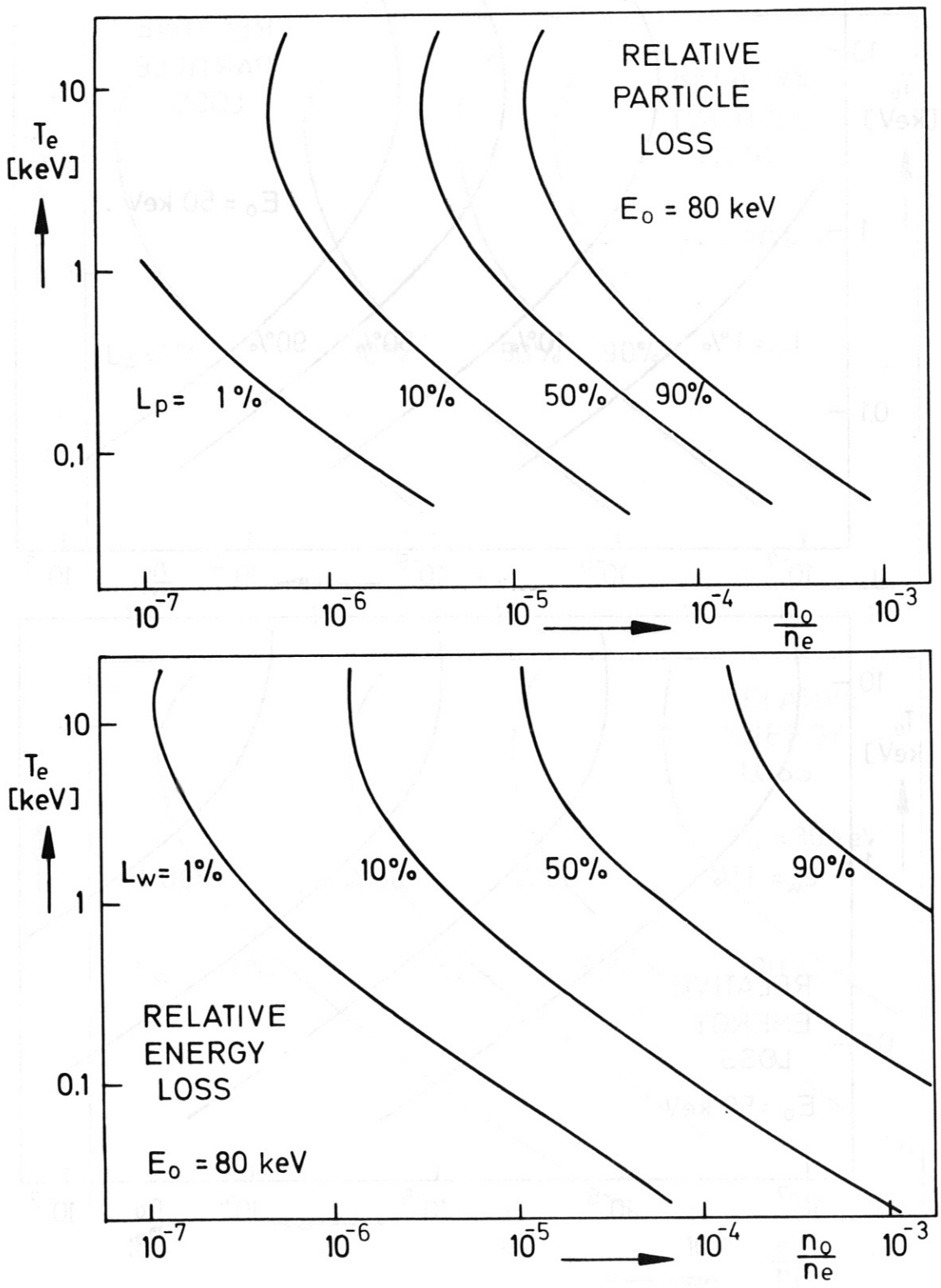
RELATIVE
PARTICLE
LOSS
E_o = 80 keV
T_e [keV]
10
1
0,1
L_p= 1%
10%
50%
90%
10^{-7}
10^{-6}
10^{-5}
10^{-4}
10^{-3}
$\frac{n_o}{n_e}$
T_e [keV]
10
1
0.1
L_w= 1%
10%
50%
90%
RELATIVE
ENERGY
LOSS
E_o = 80 keV
10^{-7}
10^{-6}
10^{-5}
10^{-4}
10^{-3}
$\frac{n_o}{n_e}$

Fig. 15

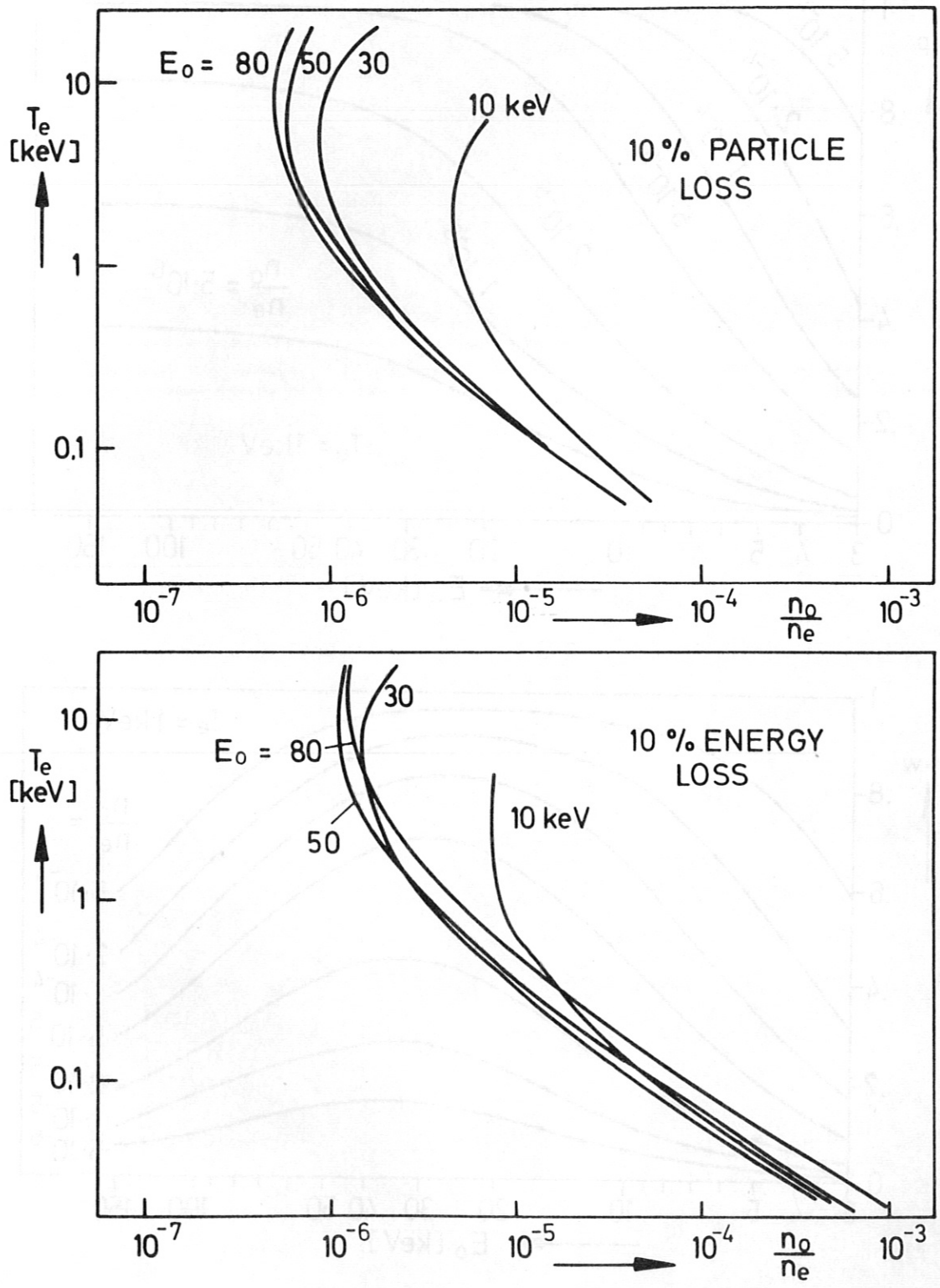
E_o = 80
50
30
10 keV
10 % PARTICLE LOSS
T_e [keV]
10
1
0.1
10^{-7}
10^{-6}
10^{-5}
10^{-4}
10^{-3}
$\frac{n_o}{n_e}$
E_o = 80
30
50
10 keV
10 % ENERGY LOSS
T_e [keV]
10
1
0.1
10^{-7}
10^{-6}
10^{-5}
10^{-4}
10^{-3}
$\frac{n_o}{n_e}$

Fig. 16

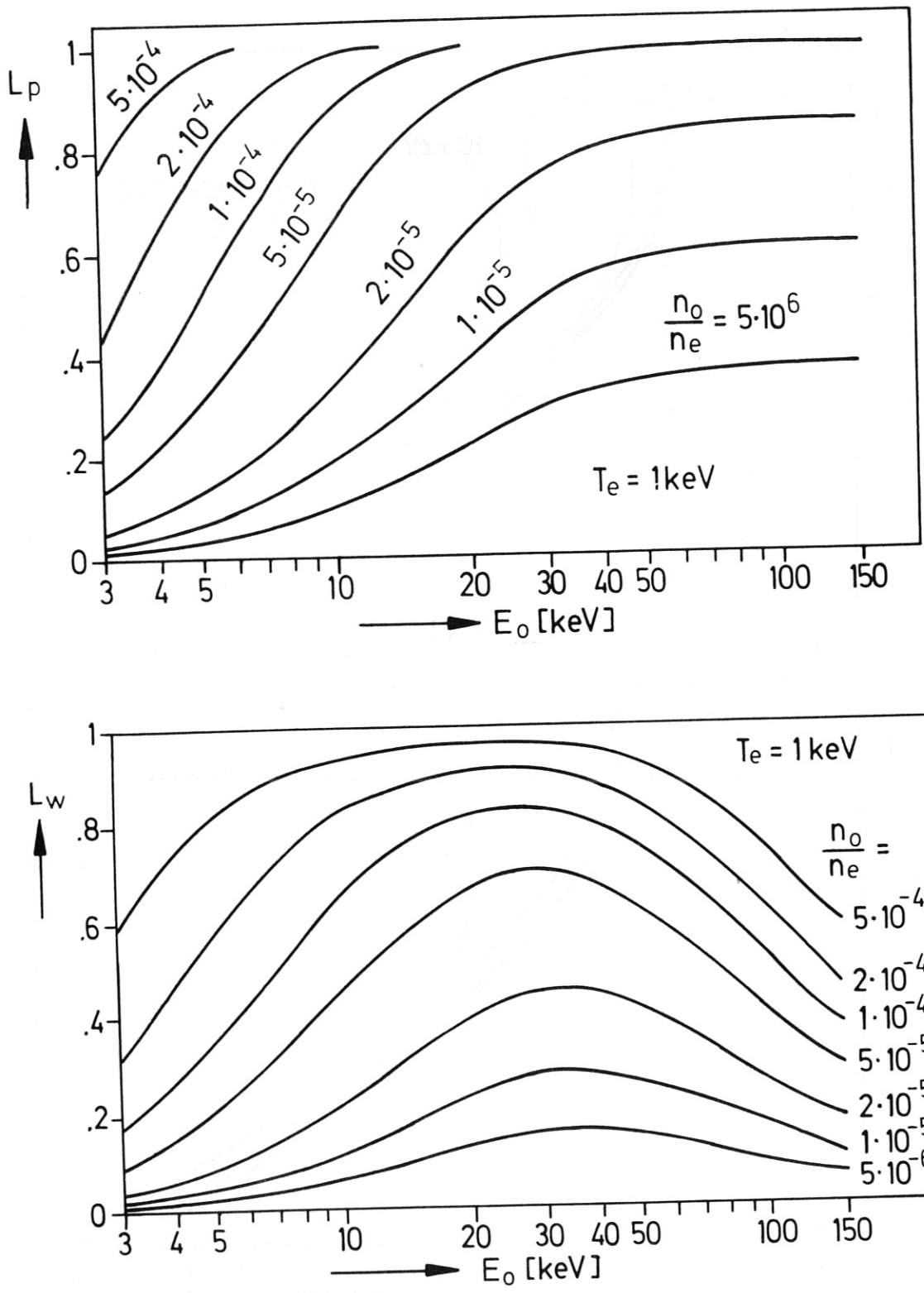
L_p
1
.8
.6
.4
.2
0
$5\cdot10^{-4}$
$2\cdot10^{-4}$
$1\cdot10^{-4}$
$5\cdot10^{-5}$
$2\cdot10^{-5}$
$1\cdot10^{-5}$
$\frac{n_o}{n_e} = 5\cdot10^{6}$
T_e = 1keV
3 4 5 10 20 30 40 50 100 150
E_o [keV]
L_w
1
.8
.6
.4
.2
0
T_e = 1 keV
$\frac{n_o}{n_e}$ =
$5\cdot10^{-4}$
$2\cdot10^{-4}$
$1\cdot10^{-4}$
$5\cdot10^{-5}$
$2\cdot10^{-5}$
$1\cdot10^{-5}$
$5\cdot10^{-6}$
3 4 5 10 20 30 40 50 100 150
E_o [keV]

Fig. 17